

Bistable and negative lateral shifts of the reflected light beam from Kretschmann configuration with nonlinear left-handed metamaterials

X. Chen · R.-R. Wei · M. Shen · Z.-F. Zhang · C.-F. Li

Received: 6 February 2010 / Revised version: 20 April 2010 / Published online: 22 May 2010
© Springer-Verlag 2010

Abstract We study the bistable and negative lateral shifts of the reflected light beam from Kretschmann configuration containing left-handed metamaterials with self-focusing and self-defocusing Kerr-type nonlinearity. It is shown that the lateral shifts can be large and negative when the thickness of the middle metal film is smaller than the critical value. Taking the nonlinear effect into account, there exists a hysteretic response between the beam shift and the intensity of the incident light beam. These results suggest that the bistable and negative beam shifts can be modulated by nonlinear coefficients and intensity of incident beam, which might be used in integrated photonics and optical switches.

1 Introduction

It is well known that the light beam totally reflected from a single interface between two different media experiences a lateral displacement with respect to the path predicted by geometrical optics. This phenomenon was called the Goos–Hänchen (GH) effect [1, 2] and theoretically explained by Artmann's stationary phase method in 1948 [3]. Because of their significant applications in electromagnetic communication system and integrated optics [4–6], the (large) negative and positive lateral shifts have been extensively investigated in partial reflection [7, 8], frustrated total internal reflection (FTIR) [9–11], and attenuated total reflection

(ATR) including Kretschmann–Raether (KR) [12–14] and Otto configurations [15–17] with various materials such as left-handed metamaterial (LHM) [18–20], weakly absorbing [21, 22], active medium [23], metal material [24], and electro-optical crystal [25]. In this regard, a relevant and surprising recent discovery is that the interplay of negative GH effect and negative refraction in the metamaterial waveguide leads to a new approach to trap rainbow, which gives rise to the applications in optical data processing and storage [26]. Therefore, these exciting prospects for manipulating light in the optical negative-index metamaterials [27] motivate one to investigate the negative and positive lateral shifts in the guide-wave configurations containing LHM.

Historically, GH shift was investigated in a single interface for total reflection, and its magnitude is only about the order of the wavelength. However, theoretical predictions and experimental verifications have shown that the lateral shifts can be large negative and positive in KR and Otto configurations due to the excitation of surface plasmas waves [12–17]. For example, Yin et al. once observed experimentally the large negative and positive lateral shift in KR configuration with thin metal film, resulting from the surface plasmon resonance. Furthermore, some recent studies have illustrated that the nonlinear surface wave (NSW) should be a more interesting topic [28–31] from the physical point of view, due to a host of new phenomena in comparison with the linear surface wave (LSW). Very recently, the bistable lateral shifts have been discovered in KR [32] and Otto [33] configurations, where the NSW can be excited at a Kerr nonlinear dielectric–metal interface. But, these studies are devoted to the NSWs for TM polarization and concentrated only on the interface of Kerr nonlinear dielectric, instead of LHM. Since the stable NSWs of TE and TM polarized can be simultaneously excited [34] and such surface waves under some conditions possesses the property of bulk NIM

X. Chen (✉) · R.-R. Wei · M. Shen · Z.-F. Zhang · C.-F. Li
Department of Physics, Shanghai University, Shanghai 200444,
P.R. China
e-mail: xchen@shu.edu.cn

X. Chen
Departamento de Química-Física, UPV-EHU, Apdo 644,
48080 Bilbao, Spain

waves, where the energy flow is directed opposite to that of the phase propagation [35], we think beyond a doubt that the lateral shifts associated with NSW in the guide-wave configurations will fuel the discovery of new phenomena as well as the development of integrated photonics and optical devices.

In this work, we will investigate theoretically the bistable and negative lateral shifts of TE-polarized light beam reflected from KR configuration containing LHM with self-focusing and self-defocusing Kerr-type nonlinearity. It is found that the lateral shifts can be large and negative based on the unique properties of NSW [34, 35], and the negative shifts can become positive with increasing the thickness of metal film. Moreover, there also exists the hysteretic response between the lateral shift and the intensity of the incident beam. Compared with the linear counterparts [13, 17], the bistable lateral shifts can be modulated by not only the incidence angle, but also nonlinear coefficients and the intensity of the incident beam. Finally, we discuss the influences of the lossy of LHM on the bistable shifts.

2 Formulation

For simplicity, we consider a TE-polarized light beam with wavelength λ and incidence angle θ_0 incident upon KR configuration containing LHM, as shown in Fig. 1, where the permittivity and permeability of the high-index prism and metal thin film are ε_1, μ_1 and ε_2, μ_2 , respectively. The permittivity and permeability of Kerr-type nonlinear LHM considered here are assumed to be $\varepsilon_3^{NL} = \varepsilon_3 + \alpha|E(z)|^2$ and μ_3 , where ε_3 is the linear part of the permittivity, and the nonlinear coefficients of self-defocusing and self-focusing nonlinearity are $\alpha = \pm|\varepsilon_3\varepsilon_0 c n_{NL}|$ with vacuum permittivity ε_0 and Kerr constant n_{NL} .

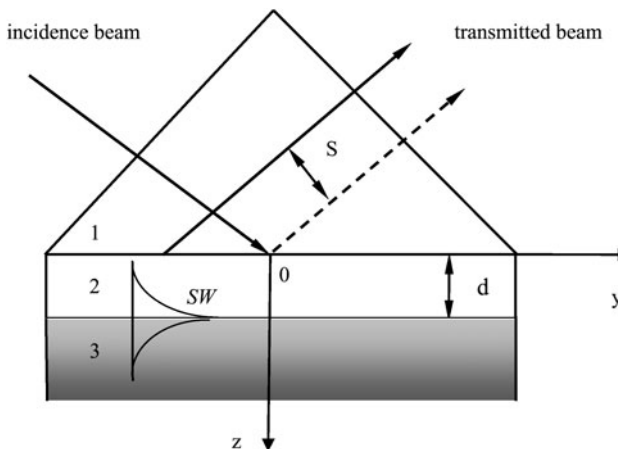


Fig. 1 Schematic diagram of the large and negative lateral shifts in KR configuration, where layers 1, 2, 3 represent high-index prism, metal film, and LHM. The incident beam, the reflected one and the excited nonlinear surface wave are also depicted

When a TE-polarized light beam is incident upon such KR configuration, the electric fields propagating in the metal film and LHM are both the evanescent waves, the NSW can thus be excited at the interface of metal film and nonlinear LHM. In this case, the nonlinear wave equation of the electric field in LHM is described by [34, 35]:

$$\frac{\partial^2 E_x(z)}{\partial^2 z} + k_0^2(\varepsilon_3 + \alpha|E_x(z)|^2 - k_y^2)E_x(z) = 0, \quad (1)$$

and k_y is the wave vector component along the nonlinear LHM interface. The solutions of the above (1) can be written as

$$E_x(z) = \begin{cases} \sqrt{\frac{2}{-|\alpha|\mu_3}} \frac{\kappa_{3z}}{k_0 \cosh[\kappa_{3z}(z-z_0)]} & \text{(self-focusing)}, \\ \sqrt{\frac{2}{-|\alpha|\mu_3}} \frac{\kappa_{3z}}{k_0 \sinh[\kappa_{3z}(z-z_0)]} & \text{(self-defocusing)}, \end{cases} \quad (2)$$

where $\kappa_{3z} = \sqrt{k_y^2 - n_3^2 k_0^2 - k_0^2 \alpha |E_x(z)|^2}$, $n_3 = -\sqrt{\varepsilon_3 \mu_3}$, k_0 is the wave vector of the vacuum, and z_0 is the position of the maximum field at the LHM interface. When the self-focusing nonlinearity is considered, the stationary surface wave has the following form:

$$E_x(z) = \begin{cases} E_d e^{i\kappa_{2z}(z-d)} e^{ik_y y} & 0 < z < d, \\ \sqrt{\frac{2}{-|\alpha|\mu_3}} \frac{\kappa_{3z}}{k_0 \cosh[\kappa_{3z}(z-d-z_0)]} e^{ik_y y} & z > d, \end{cases} \quad (3)$$

where $\kappa_{2z} = \sqrt{k_y^2 - n_2^2 k_0^2}$ and z_0 is given by

$$z_0 = \frac{1}{\kappa_{3z}} \cosh^{-1} \left[\sqrt{\frac{2}{-|\alpha|\mu_3}} \frac{\kappa_{3z}}{k_0 |E_d|} \right], \quad (4)$$

with $|E_d|$ being the amplitude of the electric field at the interface $z = d$. According to the boundary conditions, the total reflectivity can be expressed as follows,

$$r = |r| e^{i\phi} = \frac{r_{12} + r_{23} \exp(2ik_{2z}d)}{1 + r_{12}r_{23} \exp(2ik_{2z}d)}, \quad (5)$$

with

$$r_{12} = \frac{k_{1z}\mu_2 - k_{2z}\mu_1}{k_{1z}\mu_2 + k_{2z}\mu_1}, \quad (6)$$

and

$$r_{23} = \frac{k_{2z}\mu_3 - k_{3z}\mu_2}{k_{2z}\mu_3 + k_{3z}\mu_2}, \quad (7)$$

where $k_{1z} = \sqrt{n_1^2 k_0^2 - k_y^2}$, $k_{2z} = ik_{2z}$, $k_{3z} = ik_{3z}$, $k_y = k_1 \sin \theta$, and θ is the incidence angle of the plane wave component under consideration. It is noted that the self-defocusing nonlinearity can be discussed in the same way. The difference in these two cases is nothing but the nonlinear coefficients α , since the solution of z_0 has no influence

on the reflection coefficients. Furthermore, once the electric field E_d is given, the value of the incident intensity I_0 is obtained by

$$I_0 = A_0 \frac{|E_d|^2}{|t|^2}, \quad (8)$$

where $A_0 = 2|n_3|\varepsilon_0 c$ [36], and the total transmissivity t is given by

$$t = \frac{t_{12}t_{23} \exp(i k_{2z} d)}{1 + t_{12}t_{23} \exp(2 i k_{2z} d)}, \quad (9)$$

with

$$t_{12} = \frac{2k_{1z}\mu_2}{k_{1z}\mu_2 + k_{2z}\mu_1}, \quad (10)$$

and

$$t_{23} = \frac{2k_{2z}\mu_3}{k_{2z}\mu_3 + k_{3z}\mu_2}. \quad (11)$$

According to the phase shift ϕ as the function of k_y , the lateral shift, which is described in Fig. 1, is determined as [3, 20],

$$s = -\frac{d\phi}{dk_{y0}}, \quad (12)$$

where the subscript 0 denotes the values taken at $\theta = \theta_0$. Obviously, the relationship between the input intensity I_0 and the lateral shift s can be constructed with the electric field E_d . In the following discussions, we will show that (5) indicates that the reflectivity $R = |r|^2$ becomes minimum due to the excitation of NSW, which will lead to bistable and negative lateral shifts.

3 Results and discussions

In this section, we will discuss the lateral shifts of the reflected beam in detail. Figure 2 shows the large and negative lateral shifts, where the parameters of high-index prism, metal film and LHM are chosen to be $\varepsilon_1 = 12.8$, $\mu_1 = 1$, $\varepsilon_2 = -18 + 0.5i$, $\mu_2 = 1$, $\varepsilon_3 = -2.8447$, $\mu_3 = -0.4551$, the self-focusing and self-defocusing nonlinear coefficients are $\alpha = \mp 1.5105 \times 10^{-11}$ with $\varepsilon_0 = 8.85 \times 10^{-12}$ F/m and $n_{NL} = 2 \times 10^{-9}$ m²/W, and $|E_d|^2 = 1.5 \times 10^{10}$ V/m. Figure 2(a) indicates that the lateral shifts for $d = 7.7 \times 10^{-8}$ m can be large and negative when the incidence angle approaches to the surface plasmon resonance (SPR) angle θ_r , due to the excitation of the NSWs. It is seen from Fig. 2(a) that the nonlinearity of the surface wave has a great impact on the lateral shifts. Compared with the results in the case of LSW [13], Fig. 2(a) demonstrates that the maximum absolute values of the negative lateral shifts can be tuned

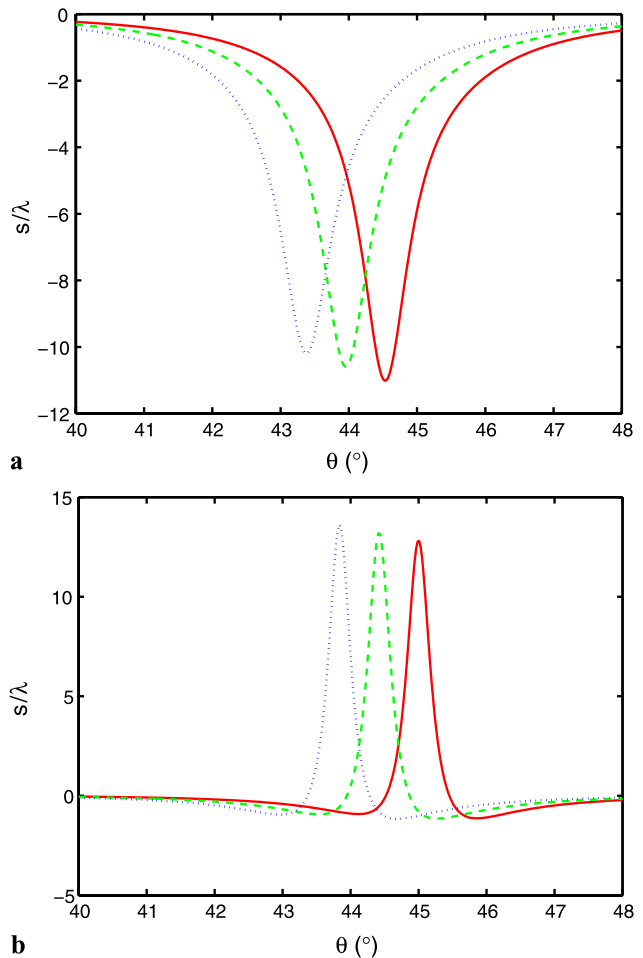


Fig. 2 Dependence of the lateral shifts on the incidence angle θ_0 , where the physical paraments are chosen to be $\lambda = 1.06 \times 10^{-6}$ m, and $|E_d|^2 = 1.5 \times 10^{10}$ V/m, (a) $d = 7.7 \times 10^{-8}$ m $< d_c$ and (b) $d = 9.4 \times 10^{-8}$ m $> d_c$. The solid, dashed, and dotted curves correspond to the cases of self-focusing nonlinearity, linearity, and self-defocusing nonlinearity

by the effective nonlinear dielectric $\varepsilon_3^{NL} = \varepsilon_3 + \alpha|E(z)|^2$, where the nonlinear coefficients $\alpha < 0$, $\alpha = 0$, and $\alpha > 0$ correspond to the self-focusing nonlinearity, linearity and self-defocusing nonlinear cases, respectively. More interestingly, Fig. 2 also illustrates that the negative lateral shifts will become positive with increasing the thickness of middle metal film. That is to say, the lateral shifts can be negative for $d < d_c$, while they become positive for $d > d_c$. This phenomenon is closely related to the properties of the reflection coefficient, $|r(\theta, d)|$, has a minimum r_{\min} in its relation with the incidence angle θ_0 at any metal film thickness d . The SPR resonance angle θ_r at which $|r|$ is minimum is dependent on the film thickness. At a particular thickness, r_{\min} becomes zero, which corresponds to the total absorption due to the dispersion relation of surface wave [17]. This partic-

ular thickness, called “critical thickness”, will play a crucial role on the sign of beam shifts and is denoted by d_c . The corresponding resonance angle at which r_{\min} is zero is denoted by θ_r^c . The critical thickness is given by

$$d_c = \frac{1}{2\text{Im}(k_{2z})} \ln \frac{|r_{23}|}{|r_{12}|}, \quad (13)$$

where θ_r^c is the solution to the following equation:

$$\phi_1 - \phi_2 - \pi = \frac{\text{Re}(k_{2z})}{\text{Im}(k_{2z})} \ln \frac{|r_{23}|}{|r_{12}|}, \quad (14)$$

which describes the resonance condition, ϕ_1 and ϕ_2 are the phase angles of r_{12} and r_{23} . Further calculations will demonstrate that $\theta_r < \theta_r^c$ for $d < d_c$, whereas $\theta_r > \theta_r^c$ for $d > d_c$. For all the parameters in Fig. 2, the critical thickness and the corresponding SPR angle are obtained as $d_c = 8.65 \times 10^{-8}$ m and $\theta_r^c = 44.84^\circ$.

In order to understand the large and negative lateral shifts discussed above, Fig. 3 shows the dependence of the reflectivity and phase shift on the incidence angle θ_0 , where the physical parameters are the same as those in Fig. 2(a). As shown in Fig. 3(a), it is clear that when the surface wave is excited around the SPR angle θ_r , the electric field can be strongly localized at the interface, thus the reflectivity approaches to a minimum value, as discussed above.

Figure 3(a) also represents that the reflectivity reaches the minimum value around the SPR angle, where $\theta_r = 43.36^\circ$ (dotted curve), $\theta_r = 43.94^\circ$ (dashed curve), and $\theta_r = 44.52^\circ$ (solid curve) correspond to the three difference cases discussed in Fig. 2(a). In addition, the drastic increase of the phase shift around θ_r , as shown in Fig. 3(b) implies the large and negative lateral shifts, according to the stationary phase theory [3]. Actually, the large and negative lateral shifts can be understood by the constructive and/or destructive interference between different plane wave components with various phase shifts. So the positive slope of phase shift for $d > d_c$ will result in the positive lateral shift. However, it is worthwhile to mention that the lateral shift for $d = d_c$ has no physical meaning, because the reflected beam in this case undergoes serious distortion, that is, stationary phase method is not valid, when the reflectivity is zero.

More importantly, there exist giant and bistable shifts with the variations of input intensity I_0 , as shown in Fig. 4(a), where $\theta_0 = 50^\circ$ and $d = 7.7 \times 10^{-8}$ m ($d < d_c$). The hysteretic behavior of lateral shifts results from the excitation of the NSW at the nonlinear LHM-metal interface. It is shown that with the intensity of incident beam increasing, the reflectivity changes slowly. When I_0 increases up to the high threshold value I_H , the reflectivity goes down with the decease of input intensity. On the contrary, the reflectivity will jump into a higher value until I_0 reaches the low threshold value I_L . This phenomenon is similar to the

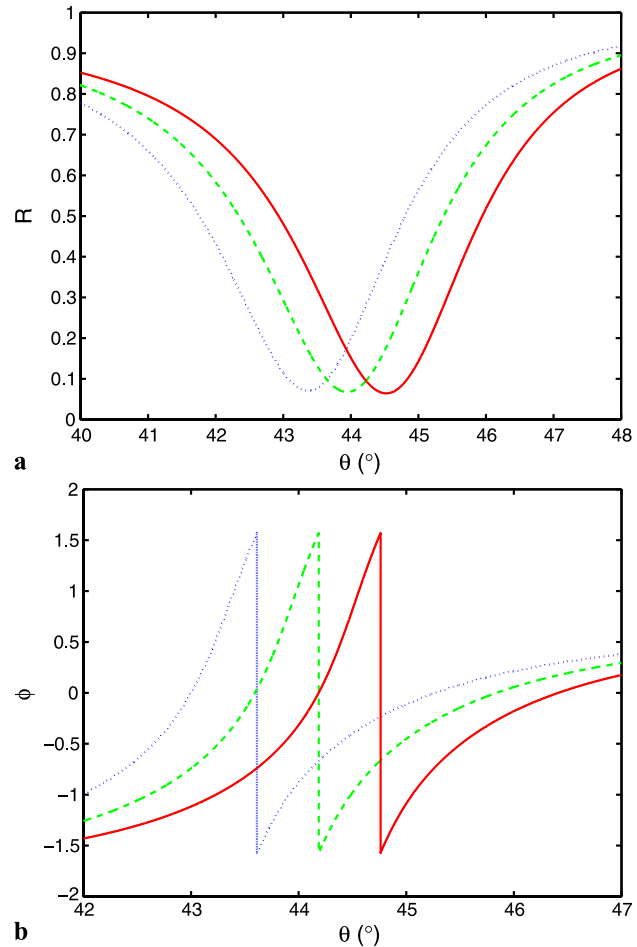


Fig. 3 Dependence of the reflectivity (a) and phase shift (b) on the incidence angle θ_0 , where the physical parameters are the same as those in Fig. 2(a). The solid, dashed, and dotted curves correspond to self-focusing nonlinearity, linear, and self-defocusing nonlinearity cases

result in similar KR configuration containing the interface between metal and nonlinear Kerr dielectric [32]. However, the behavior of bistable shift is quite different. With the input intensity increasing, the bistable shift decreases slowly, but when I_0 is up to the high threshold value I_H , the negative shift will jump into the smaller one, corresponding to a larger absolute value of the lateral shift. Compared with the result that the negative lateral shift increases slightly with the decrease of input intensity, the negative shift sharply decreases to a very small absolute value until I_0 reaches the low threshold value I_L , which corresponds to the peak shown in Fig. 4(a). But Fig. 4(b) shows that the hysteretic behavior of the lateral shift will disappear for $d > d_c$.

Figure 5(a) and (b) further demonstrate the dependence of the bistable shifts on input intensity I_0 at various incidence angles in the cases of self-focusing and self-defocusing nonlinearity, where (a) $\theta_0 = 50^\circ$ (solid curve), $\theta_0 = 48^\circ$ (dashed curve), $\theta_0 = 46^\circ$ (dotted curve), (b) $\theta_0 = 40^\circ$ (solid curve), $\theta_0 = 38^\circ$ (dashed curve), $\theta_0 = 36^\circ$ (dot-

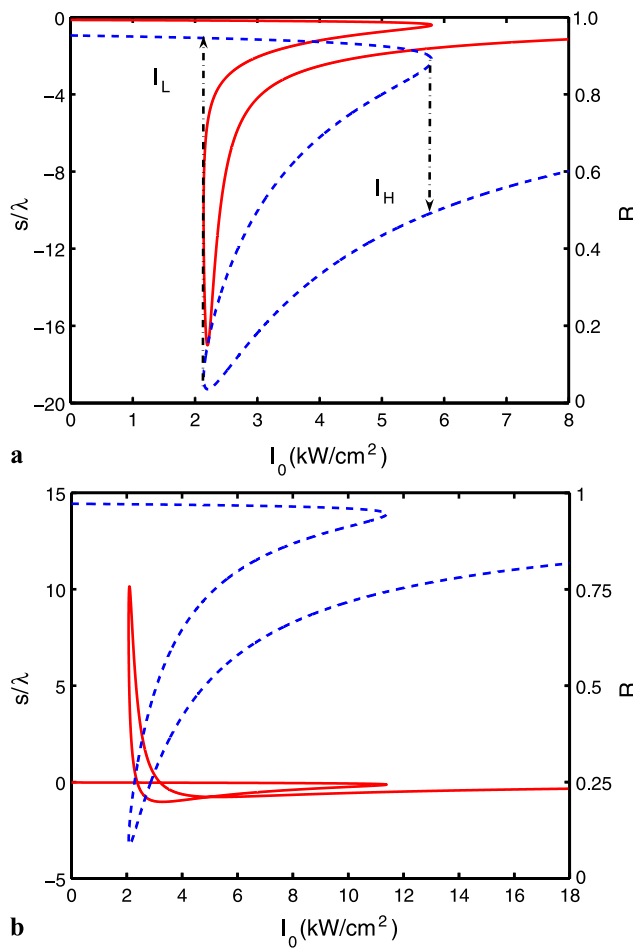


Fig. 4 Dependence of the bistable lateral shift (solid curves) and reflectivity (dashed curves) on the intensity I_0 of incident beam in the case of self-focusing nonlinearity, where $\theta_0 = 50^\circ$, (a) $d = 7.7 \times 10^{-8}$ m, (b) $d = 9.4 \times 10^{-8}$ m, and the other parameters are the same as those in Fig. 2

ted curve), the other parameters are the same as those in Fig. 2. It is implied that the high threshold values I_H are more sensitive to θ_0 than the low threshold values I_L . For the certain thickness of metal film $d = 7.7 \times 10^{-8}$ m, the hysteretic behavior of the lateral shift in the case of self-focusing nonlinearity will disappear with the decrease of incidence angle. And the peak of the lateral shifts also becomes larger when increasing incidence angle θ_0 slightly. On the contrary, Fig. 5(b) shows that the hysteretic behavior of beam shift in the case of self-defocusing nonlinearity will disappear, when the incidence angle θ_0 becomes larger. All these interesting phenomena on the bistable and negative lateral shifts can be applicable to design spatial modulation and optical switch.

Finally, we would like to discuss the influence of loss on the bistable shifts, because the real metamaterial has unavoidable losses. To this end, the dielectric permittivity and magnetic permeability of LHM are taken to be complex numbers, $\varepsilon = \varepsilon_3^{NL} + i\varepsilon_i$ and $\mu = \mu_3 + i\mu_i$, where ε_3^{NL} , ε_i , μ_3 ,

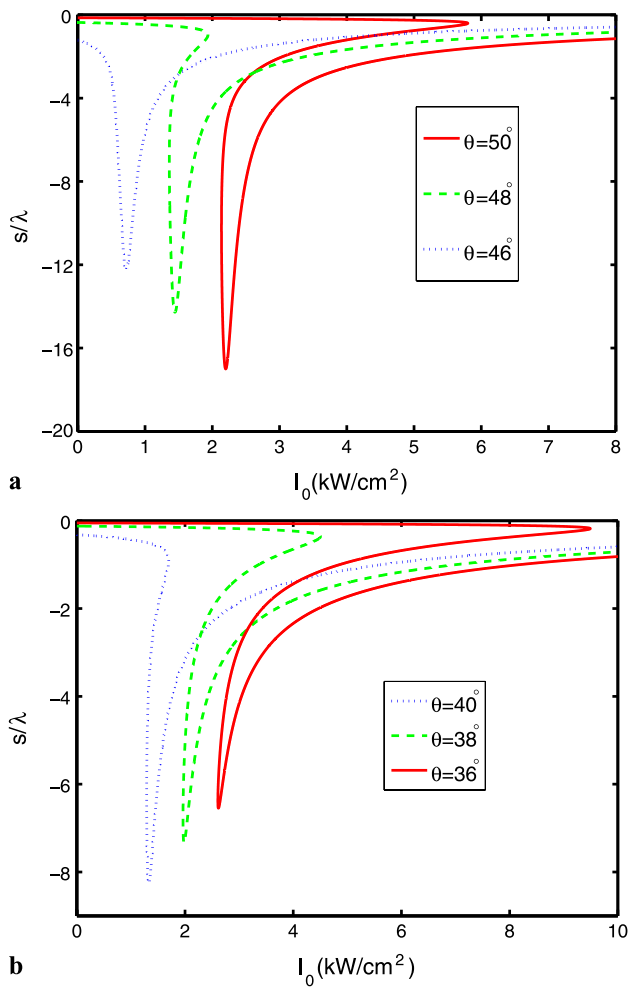


Fig. 5 Dependence of the bistable shifts on the input intensity I_0 at various incidence angles θ_0 in the cases of (a) self-focusing and (b) self-defocusing nonlinearity, where (a) $\theta_0 = 50^\circ$ (solid curve), $\theta_0 = 48^\circ$ (dashed curve), $\theta_0 = 46^\circ$ (dotted curve), (b) $\theta_0 = 40^\circ$ (solid curve), $\theta_0 = 38^\circ$ (dashed curve), $\theta_0 = 36^\circ$ (dotted curve), and the other parameters are the same as those in Fig. 2

and μ_i are all the real number. For the sake of simplification, we assume here that ε_i and μ_i have the same values. Figure 6 shows that the dependence of the bistable shifts on the input intensity I_0 with different losses of the metamaterial in the cases of (a) self-focusing and (b) self-defocusing nonlinearity, where (a) $\theta_0 = 50^\circ$, $\varepsilon_i = \mu_i = 0.001$ (solid curve), $\varepsilon_i = \mu_i = 0.003$ (dashed curve), $\varepsilon_i = \mu_i = 0.005$ (dotted curve), $\varepsilon_i = \mu_i = 0.008$ (dash-dotted curve), (b) $\theta_0 = 38^\circ$, $\varepsilon_i = \mu_i = 0.001$ (solid curve), $\varepsilon_i = \mu_i = 0.005$ (dashed curve), $\varepsilon_i = \mu_i = 0.010$ (dotted curve), $\varepsilon_i = \mu_i = 0.015$ (dashed-dotted curve), the other parameters are the same as those in Fig. 2. It is shown in Fig. 6 that the bistable shifts still survive for the weakly lossy LHM. Comparisons of Fig. 6 and Fig. 5 further suggest that the weak absorbing LHM will enlarge the absolute value of the negative lateral shifts. But the lateral shift will be changed from negative to positive with increasing ε_i and μ_i . Actually, with enough

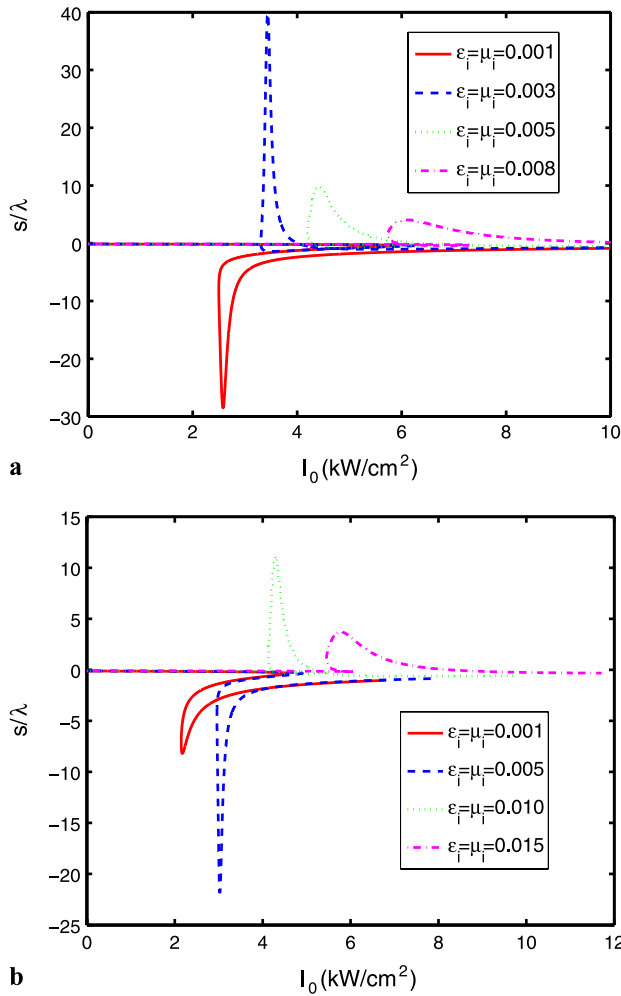


Fig. 6 Dependence of the bistable shifts on the input intensity I_0 with different losses of the metamaterial in the cases of (a) self-focusing and (b) self-defocusing nonlinearity, where (a) $\theta_0 = 50^\circ$, $\varepsilon_i = \mu_i = 0.001$ (solid curve), $\varepsilon_i = \mu_i = 0.003$ (dashed curve), $\varepsilon_i = \mu_i = 0.005$ (dotted curve), $\varepsilon_i = \mu_i = 0.008$ (dash-dotted curve), (b) $\theta_0 = 38^\circ$, $\varepsilon_i = \mu_i = 0.001$ (solid curve), $\varepsilon_i = \mu_i = 0.005$ (dashed curve), $\varepsilon_i = \mu_i = 0.010$ (dotted curve), $\varepsilon_i = \mu_i = 0.015$ (dashed-dotted curve), and the other parameters are the same as those in Fig. 2

large ε_i and μ_i , the loss of LHM will ruin gradually the hysteretic characteristic of lateral shifts. In addition, Fig. 6 also shows that the loss of LHM with self-focusing nonlinearity is more sensitive to the beam shift than that with self-defocusing nonlinearity.

4 Conclusion

In summary, we have investigated the giant bistable and negative lateral shifts for TE-polarized light beam reflected from KR configuration containing LHM with self-focusing and self-defocusing Kerr-type nonlinearity. Due to the excitation of the NSW in the LHM, the lateral shifts can be enhanced, and become negative when the incidence angle θ_0

is around the SPW angles. It is worth pointing out that the lateral shifts will change from negative to positive, when the thickness of metal film is satisfied $d > d_c$. Taking the self-focusing and self-defocusing Kerr-type nonlinearity into account, we have also found that there exist hysteretic phenomena of lateral shifts and their corresponding reflectivity with various I_0 and incidence angle θ_0 . It is clear that the modulation of the lateral shifts can be realized via changing incidence angle, nonlinear coefficients, and input intensity of light beam. In addition, the influence of the loss of a real metamaterial on the bistable shift are also discussed in both cases of self-focusing and self-defocusing Kerr-type nonlinearity. Finally, it should be emphasized here that we can consider the giant and bistable lateral shifts of TM-polarized light beam in the same way. However, it is because the interface associated with LHM can support both TE- and TM-polarized surface waves that the large positive or negative lateral shifts will be simultaneously realized for TE and TM-polarized light beams in the similar configuration containing LHM as we consider here. This is also potentially useful to design new type of polarization beam splitter. With the recent advances of nonlinear effects in metamaterials in microwave and even optical frequencies [37], we hope that all these phenomena discussed here may lead to some potential applications in integrated optics and optical devices.

Acknowledgements This work is supported by the National Natural Science Foundation of China (Grant Nos. 60806041, 60808002, and 60877055), the Shanghai Rising-Star Program (Grant No. 08QA14030), the Shanghai Educational Development Foundation (Grant No. 2007CG52), the Science and Technology Commission of Shanghai (Grant No. 08JC14097), and the Shanghai Leading Academic Discipline Program (S30105). X.C. acknowledges Juan de la Cierva Programme and FIS2009-12773-C02-01. R.R.W. thanks the Innovation Fund of Shanghai University for graduate student (Grant No. SHUCX092023).

References

1. F. Goos, H. Hänchen, Ann. Phys. **1**, 333 (1947)
2. F. Goos, H. Hänchen, Ann. Phys. **5**, 251 (1949)
3. K.V. Artmann, Ann. Phys. (Leipz.) **2**, 87 (1948)
4. H.K.V. Lotsch, Optik (Stuttg.) **32**, 116 (1970)
5. H.K.V. Lotsch, Optik (Stuttg.) **32**, 189 (1970)
6. H.K.V. Lotsch, Optik (Stuttg.) **32**, 299 (1970)
7. C.W. Hsue, T. Tamir, J. Opt. Soc. Am. A **2**, 978 (1985)
8. C.F. Li, Phys. Rev. Lett. **91**, 133903 (2003)
9. A.K. Ghatak, M.R. Shenoy, I.C. Goyal, K. Thyagarajan, Opt. Commun. **56**, 313 (1986)
10. A. Haibel, G. Nimtz, A.A. Stahlhofen, Phys. Rev. E **63**, 047601 (2001)
11. X. Chen, C.-F. Li, R.-R. Wei, Y. Zhang, Phys. Rev. A **80**, 015803 (2009)
12. S.L. Chuang, J. Opt. Soc. Am. **3**, 593 (1986)
13. X.B. Yin, L. Hesselink, Z. Liu, N. Fang, X. Zhang, Appl. Phys. Lett. **85**, 372 (2004)
14. L.G. Wang, S.Y. Zhu, Appl. Phys. Lett. **87**, 221102 (2005)
15. I.V. Shadrivov, A.A. Zharov, Y.S. Kivshar, Appl. Phys. Lett. **83**, 2713 (2003)

16. I.V. Shadrivov, R.W. Ziolkowski, A.A. Zharov, Y.S. Kivshar, Opt. Express **13**, 481 (2005)
17. S.M. Vuković, N.B. Aleksić, D.V. Timotijevića, Eur. Phys. J. D **39**, 295 (2006)
18. P.R. Berman, Phys. Rev. E **66**, 067603 (2002)
19. A. Lakhtakia, Electromagnetics **23**, 71 (2003)
20. X. Chen, C.-F. Li, Phys. Rev. E **69**, 066617 (2004)
21. L.G. Wang, H. Chen, S.Y. Zhu, Opt. Lett. **30**, 2936 (2005)
22. L.G. Wang, S.Y. Zhu, J. Appl. Phys. **98**, 043522 (2005)
23. J. Fan, L.J. Wang, Opt. Commun. **259**, 149 (2006)
24. M. Merano, A. Aiello, G.W. Hooft, M.P. van Exter, E.R. Eliel, J.P. Woerdman, Opt. Express **15**, 15928 (2007)
25. X. Chen, M. Shen, Z.-F. Zhang, C.-F. Li, J. Appl. Phys. **104**, 123101 (2008)
26. K.L. Tsakmakidis, A.D. Boardman, O. Hess, Nature (Lond.) **450**, 397 (2007)
27. V.M. Shalaev, Nat. Photonics **1**, 41 (2006)
28. G.M. Wysin, H.J. Simon, R.T. Deck, Opt. Lett. **6**, 30 (1981)
29. I.I. Smolyaninov, Phys. Rev. Lett. **94**, 057403 (2005)
30. J.-H. Huang, R.-L. Chang, P.-T. Leung, D.-P. Tsai, Opt. Commun. **282**, 1412 (2009)
31. G.-D. Xu, T. Pan, T.-C. Zang, J. Sun, J. Phys. D, Appl. Phys. **42**, 045303 (2009)
32. H.C. Zhou, X. Chen, P. Hou, C.F. Li, Opt. Lett. **33**, 1249 (2008)
33. K. Kim, D.K. Phung, F. Rotermund, H. Lim, Opt. Express **16**, 15506 (2008)
34. I.V. Shadrivov, A.A. Sukhorukov, Y.S. Kivshar, A.A. Zharov, A.D. Boardman, P. Egan, Phys. Rev. E **69**, 016617 (2004)
35. S.A. Darmanyan, M. Nevière, A.A. Zakhidov, Phys. Rev. E **72**, 036615 (2005)
36. R.W. Boyd, *Nonlinear Optics* (Academic Press, San Diego, 2003), p. 568
37. W.-S. Cai, V. Shalaev, *Optical Metamaterials: Fundamentals and Applications* (Springer, Berlin, 2009). Chap. 7 and references therein